PARTICLE AND RESONANCE PRODUCTION IN $\bar{p}p$ INTERACTIONS AT 12 GeV/c*

D. Gall, M. Penna†, G. Wetjen and V. Blobel

II. Institut für Experimentalphysik der Universität Hamburg

and

Deutsches Elektronen-Synchrotron DESY, Hamburg

(Received 19th August 1975)

ABSTRACT

We present data on multiplicities and inclusive particle and resonance production in $\bar{p}p$ interactions at 12 GeV/c. These data are from an older exposure[1] of the CERN 2m hydrogen bubble chamber; all topologies were remeasured with an HPD. A total number of about 25000 events were analysed. The results will be compared with results for pp collisions at the same energy, which have also been studied in our laboratory[2]. Identical experimental procedures were employed in these two experiments.

---

* Work supported by the Bundesministerium für Forschung und Technologie.

† On leave from Centro Brasileiro de Pesquisas Físicas, Rio de Janeiro.

1. Integrated Cross Sections and Multiplicities

The total cross sections and charged particle multiplicities are given in Table 1. The total inelastic cross sections for pp and $\bar{p}p$ differ of course. Also the multiplicity $\langle n_{ch} \rangle$, the dispersion parameter D^2 and the correlation parameter f_2 are different[3]. It is more meaningful to compare only the non-annihilation part of the $\bar{p}p$ interactions with the pp interaction. Differences between these two interactions are due to interference effects[4], which can be expected to get averaged out in integrated quantities like total cross sections and multiplicities.

	total	$\bar{p}p$ annihilation	non-annihilation	pp
σ_{tot}	51.7±0.8 mb			39.6±0.1 mb
σ_{tot}^{inel}	40.1±0.9 mb	12.3±1.4 mb	27.8±1.3 mb	29.75±0.25 mb
$\langle n_{ch} \rangle$	4.05±0.08	5.49±0.14	3.42±0.10	3.43±0.03
$D^2=\langle n_{ch}^2 \rangle - \langle n_{ch} \rangle^2$	3.96±0.14	3.77±0.32	2.73±0.25	2.05±0.03
$f_2=D^2-\langle n_{ch} \rangle$	-0.09±0.14	-1.72±0.32	-0.69±0.22	-1.38±0.04

Table 1. Total cross sections and multiplicity parameters for $\bar{p}p$ and pp interactions at 12 GeV/c

Separation of annihilation from non-annihilation channels is experimentally difficult, in particular the separation between annihilation and final states with $\bar{n}n$. To get an event-by-event separation of annihilation and non-annihilation, we have applied to our data a procedure similar to the one used successfully at 4.6 and 9.1 GeV/c[5]. The amount of annihilation within the sample of

events which were ambiguous between annihilation and final states with $\bar{n}n$ was determined in the following way: To the missing mass distribution for each topology we fitted a sum of distributions for the effective mass of two and more pions and of two nucleons and pions, taken from (4C- and 1C-) fit channels of higher topologies; it was verified that the results for each topology were compatible with the inclusive π^0 cross section obtained from the observed e^+e^---pair creation probability. From the fits a cut in missing mass was determined which yields the fitted amount of annihilation; the cut is at about 2.5 to 3.0 GeV, depending on topology.

Results obtained with this separation are also shown in Table 1. For non-annihilation the total inelastic cross section of 27.8 ± 1.3 mb as well as the charged multiplicity are compatible with the pp data. Annihilation has a cross section of 12.3±1.4 mb and a significantly larger charged multiplicity.

The topological cross sections for inelastic $\bar{p}p$ and pp interactions are shown in Fig. 1. The $\bar{p}p$ non-annihilation cross sections agree within errors with the pp topological cross sections.

2. Inclusive Particle Production in Non-Annihilation Processes

We now discuss the inclusive non-annihilation processes

$$\bar{p} + p \rightarrow p + \text{anything} \qquad (1)$$

and

$$\bar{p} + p \rightarrow \pi^{\pm} + \text{anything} \qquad (2)$$

(i.e. the anything containing at least one antibaryon).
The invariant cross section for reaction (1) is shown as a function

of Feynman's x variable integrated over transverse momentum p_T in Fig. 2 and for several values of transverse momentum p_T in Fig. 3.

p production extends only up to about x = + 0.3 into the region of positive x. Shown as curves in Figs. 2 and 3 are the corresponding cross sections for pp interactions, where of course target and beam fragmentation add in the region $-0.3 < x < +0.3$. In Fig. 4 the sum of the p and $\bar{p}$ distributions (the $\bar{p}$ distribution is obtained from the p distribution by a CP transformation which is simply a reflection of the p distribution at x = 0) is compared with the pp data. Whereas there is rough agreement in the region of small $|x|$, in the diffractive region of large $|x|$ some differences are apparent.

For pion production (reaction (2)) the invariant cross sections integrated over transverse momentum p_T are shown in Fig. 5, together with the analogous distribution from pp collisions. In the target (beam) fragmentation region the distributions for pions of charge equal to the target (beam) are of similar shape, e.g. π^+ from pp and π^+ from $\bar{p}p$ interactions in the target fragmentation region, and π^+ from pp and π^- from $\bar{p}p$ interactions in the beam fragmentation region. The same is true for pions of charge opposite to the target (beam). The agreement in magnitude is better for the latter case.

In Fig. 6 the p_T^2 distribution of the inclusive pion production in reaction (2) is shown. The fall with increasing p_T^2 up to $p_T^2 = 0.5\ \mathrm{GeV}^2$ is similar to that observed for pions in pp collisions (shown as curves).

3. Pion Production in Annihilation Processes

We now study pion production in annihilation processes

$$\bar{p} + p \rightarrow \pi^{\pm} + \text{anything} \qquad (3)$$

(i.e. the anything containing no baryons or antibaryons). The x distribution of the pions shown in Fig. 7 is wider than for the non-annihilation events (Fig. 5). On the average the longitudinal momentum of the pions in the c.m. is larger for annihilation than for non-annihilation processes. In Table 2 the mean values of the transverse momenta for inclusive pion production (and p production) in $\bar{p}p$ and pp interactions are given. In Fig. 8 we compare the cross sections for annihilation and non-annihilation as a function of p_T^2. For annihilation the cross section decreases more slowly with increasing p_T^2, such that the average transverse momentum is larger in annihilation than in non-annihilation.

	$\bar{p}p$ total	$\bar{p}p$ annihilation	$\bar{p}p$ non-annihilation	pp
π	319 ± 1	361 ± 2	284 ± 2	π^+ 309.7 ± 0.7 π^- 296.3 ± 0.3
p	408 ± 4	——	408 ± 4	393.9 ± 0.4

Table 2. Mean values of transverse momentum in MeV/c for $\bar{p}p$ and pp interactions at 12 GeV/c.

This feature is shown in more detail in Fig. 9. Here $\langle p_T \rangle$ is plotted against the average $\langle |p_L^*| \rangle$ of the absolute value of the longitudinal momentum in the c.m. for pions in several exclusive final states. Shown also are corresponding values for non-anni

hilation final states with 2 to 10 charged particles and, as a straight line, the dependence for isotropic distribution in the c.m. The difference between annihilation and non-annihilation is largest for channels of low pion multiplicity, as has already been observed at other energies[6]. It was verified that this less peripheral nature of annihilation is not caused by the decay of heavy resonances (ρ, f, ...).

4. Inclusive Production of Vector Mesons

Clear ρ^0 signals are seen in the distributions of effective mass of all $\pi^+\pi^-$ combinations shown in Fig. 10 for the total event sample and the annihilation sample. The ρ^0 production cross sections in the inclusive reaction

$$\bar{p} + p \rightarrow \rho^0 + \text{anything} \qquad (4)$$

obtained from independent fits to the mass distributions (total, annihilation, non-annihilation) are given in Table 3. The total ρ^0 cross section of 6.5 ± 0.5 mb is much larger than in pp interactions, where the cross section is 1.80 ± 0.25 mb at 12 GeV/c[7] (the methods of fitting resonance and background are identical in both experiments). A very important contribution of 4.4 ± 0.4 mb is from annihilation. For annihilation into pions the total inclusive cross section is $\sigma(\pi) \simeq 3\sigma(\pi^0)$ and it is reasonable to assume also $\sigma(\rho) \simeq 3\sigma(\rho^0) = 13.2$ mb. With $\sigma(\pi) \simeq 103$ mb it follows that more than 1/4 of all pions are from ρ decay. The non-annihilation ρ^0 cross section is compatible with the pp value.

final state	total	$\bar{p}p$ annihilation	non-annihilation	pp
ρ^0+anything	6.5±0.5 mb	4.4±0.4 mb	2.1±0.4 mb	1.80±0.25mb
ω+charged part.	0.56±0.06mb	0.25±0.05mb	0.31±0.04mb	0.32±0.02mb

Table 3. Cross sections for production of vector mesons in $\bar{p}p$ and pp interactions at 12 GeV/c.

ω production can only be studied in our experiment in quasi-inclusive processes

$$\bar{p} + p \rightarrow \omega + \text{charged particles} \qquad (5)$$

In Fig. 11 the distributions of effective mass of the $\pi^+\pi^-\pi^0$ combinations are shown for the total event sample and for non-annihilation. The cross sections for ω production in reaction (5) are also shown in Table 3. Again the cross section values for non-annihilation and pp interactions are compatible. The relatively small ω cross section for annihilation may result from the fact that most often neutral particles are produced together with the ω ; therefore the data do not indicate that inclusive ω production is much weaker than ρ^0 production.

Fig. 12 and 13 show the cross sections as a function of rapidity y^* and as a function of p_T^2 for ρ^0 and ω production in reactions (4) and (5) from the total event sample. Also shown are the corresponding data for pp interactions. The distributions for both kinds of initial states are of similar form, the ρ^0 and ω being produced mainly centrally. The p_T^2 distributions can be approximated by an exponential; the values for the slope are (4.1±0.4) GeV^{-2} and

(3.2 ± 0.4) GeV^{-2} for ρ^0 and ω production, respectively.

ACKNOWLEDGEMENT

We thank Prof. Cresti for his help in obtaining the film, Dr. Drews for helpful information on the earlier analysis of this experiment and Prof. Söding for stimulating discussions.

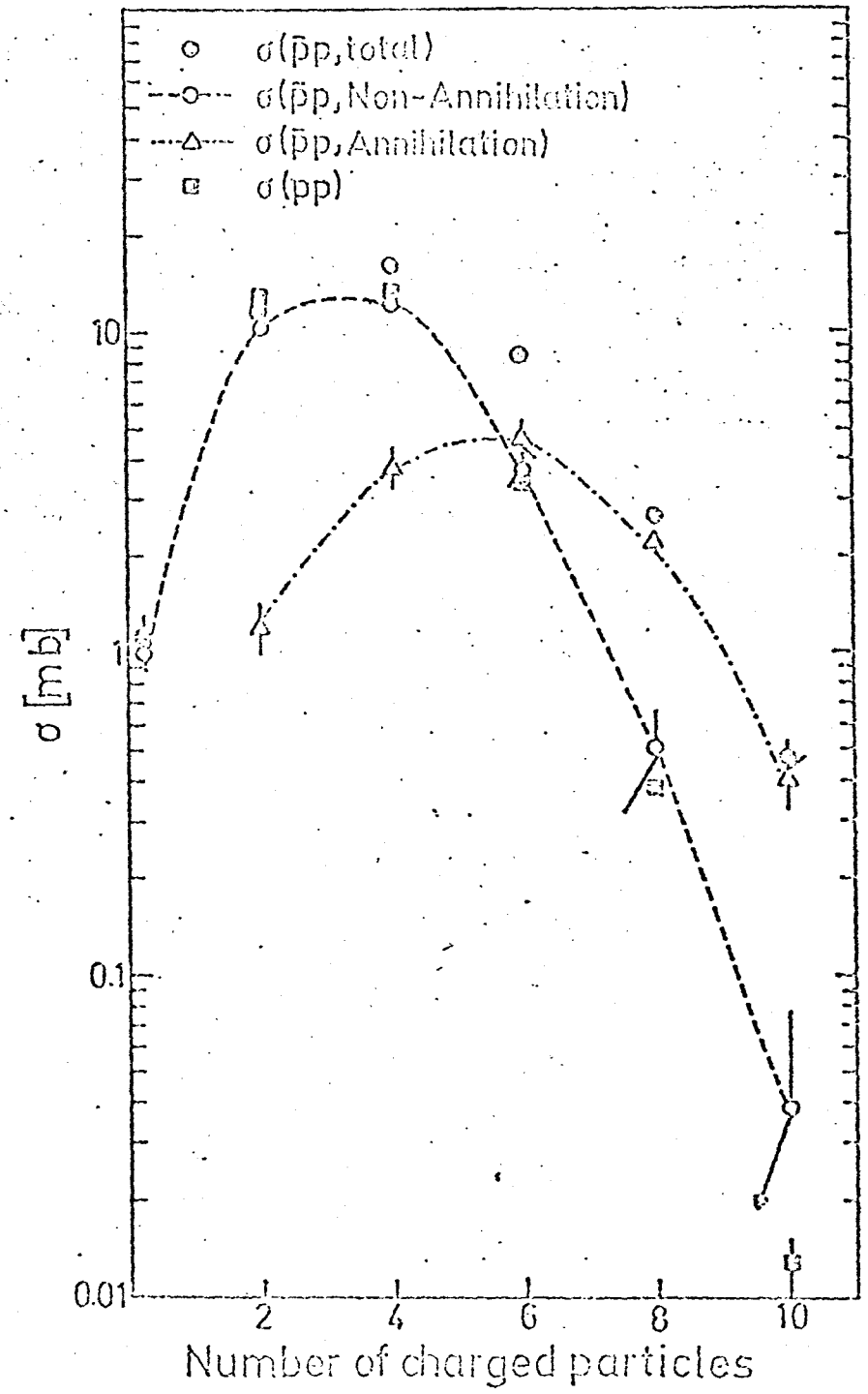
σ(p̄p,total)
σ(p̄p,Non-Annihilation)
σ(p̄p,Annihilation)
σ(pp)
10
1
0.1
0.01
σ [mb]
2
4
6
8
10
Number of charged particles

Fig. 1

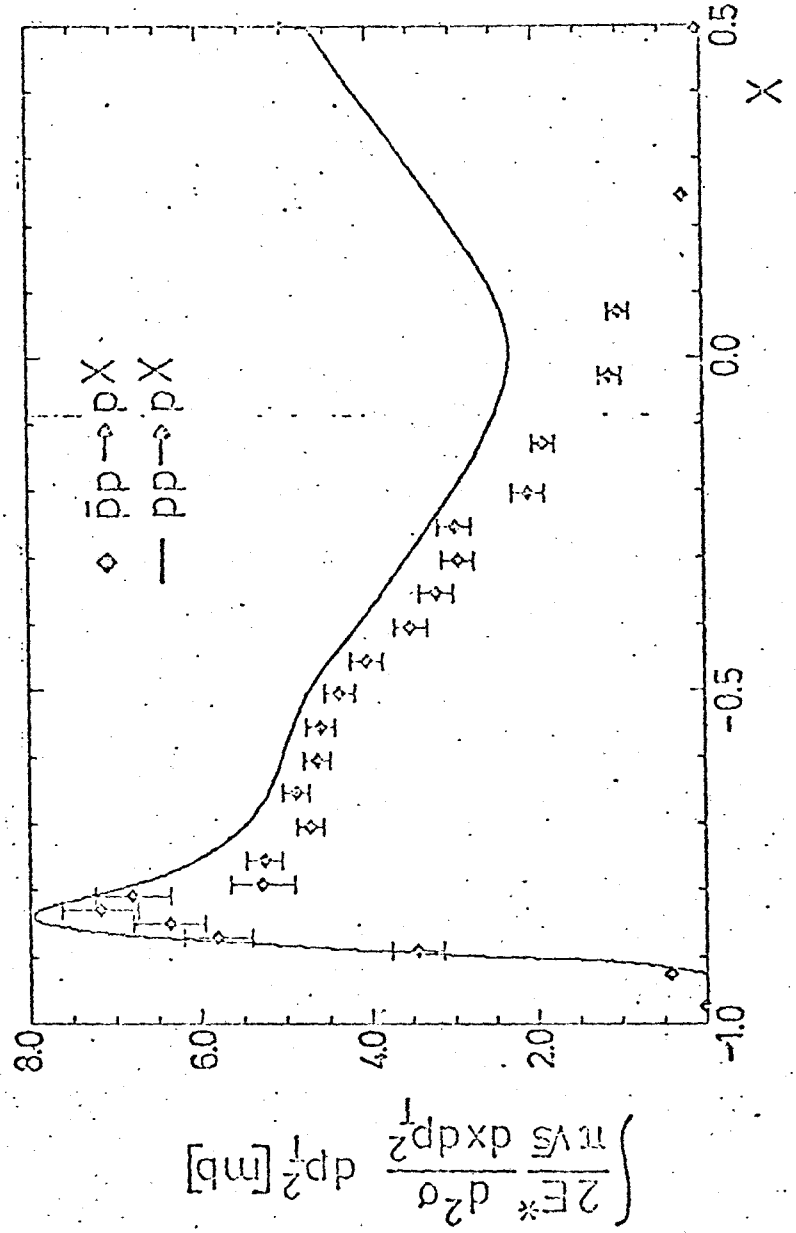
$\int \frac{2E^*}{\pi V_S} \frac{d^2\sigma}{dx dp_T^2} dp_T^2$ [mb]
8.0
6.0
4.0
2.0
-1.0
-0.5
0.0
0.5
X
pp → dX
p̄p → dX

Fig. 2

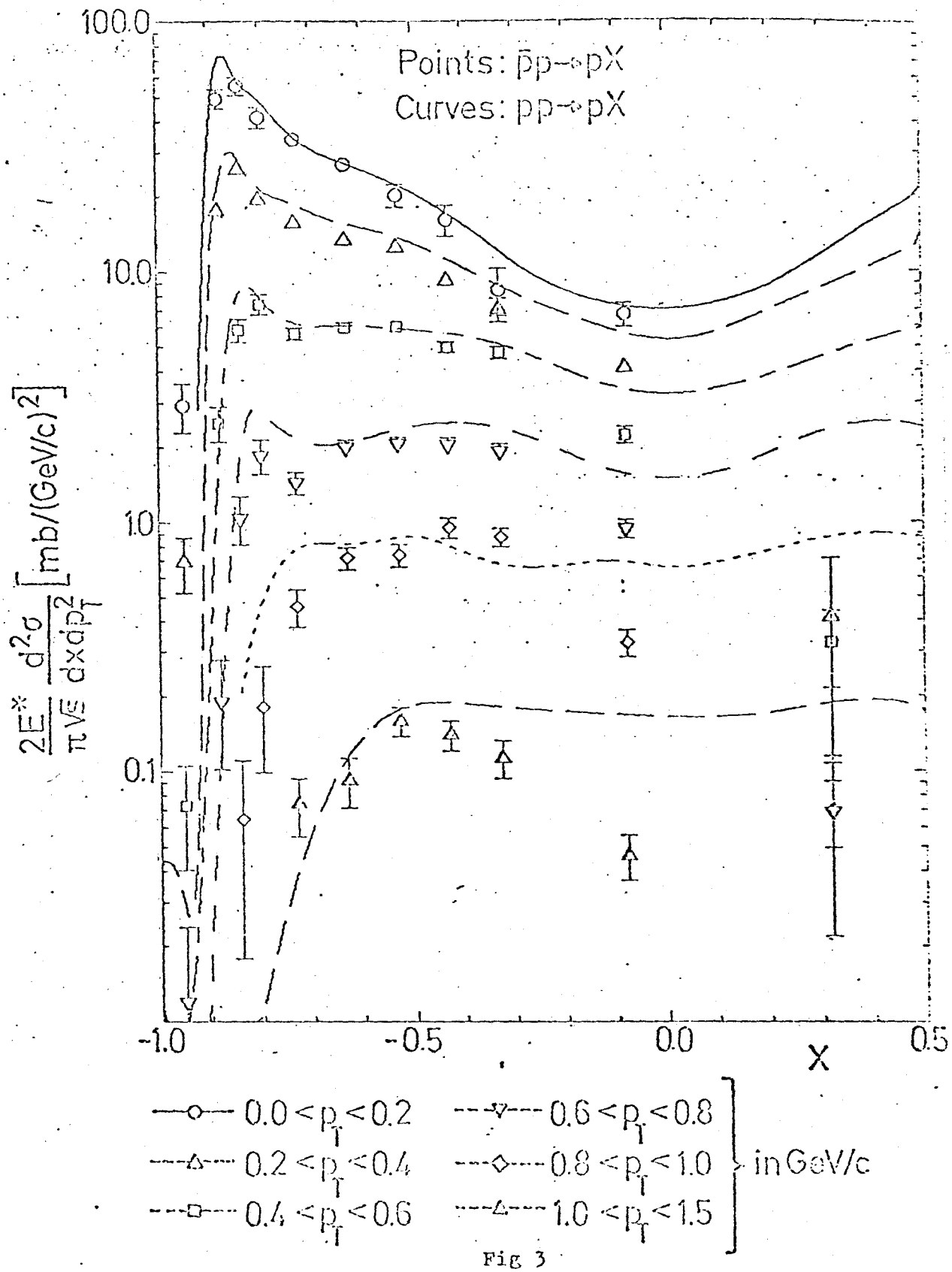
Points: $\bar{p}p \to pX$
Curves: $pp \to pX$
$\frac{2E^*}{\pi\sqrt{s}} \frac{d^2\sigma}{dx\,dp_T^2}$ [mb/(GeV/c)^2]
100.0
10.0
1.0
0.1
-1.0
-0.5
0.0
0.5
X
$0.0 < p_T < 0.2$
$0.2 < p_T < 0.4$
$0.4 < p_T < 0.6$
$0.6 < p_T < 0.8$
$0.8 < p_T < 1.0$
$1.0 < p_T < 1.5$
} in GeV/c

Fig 3

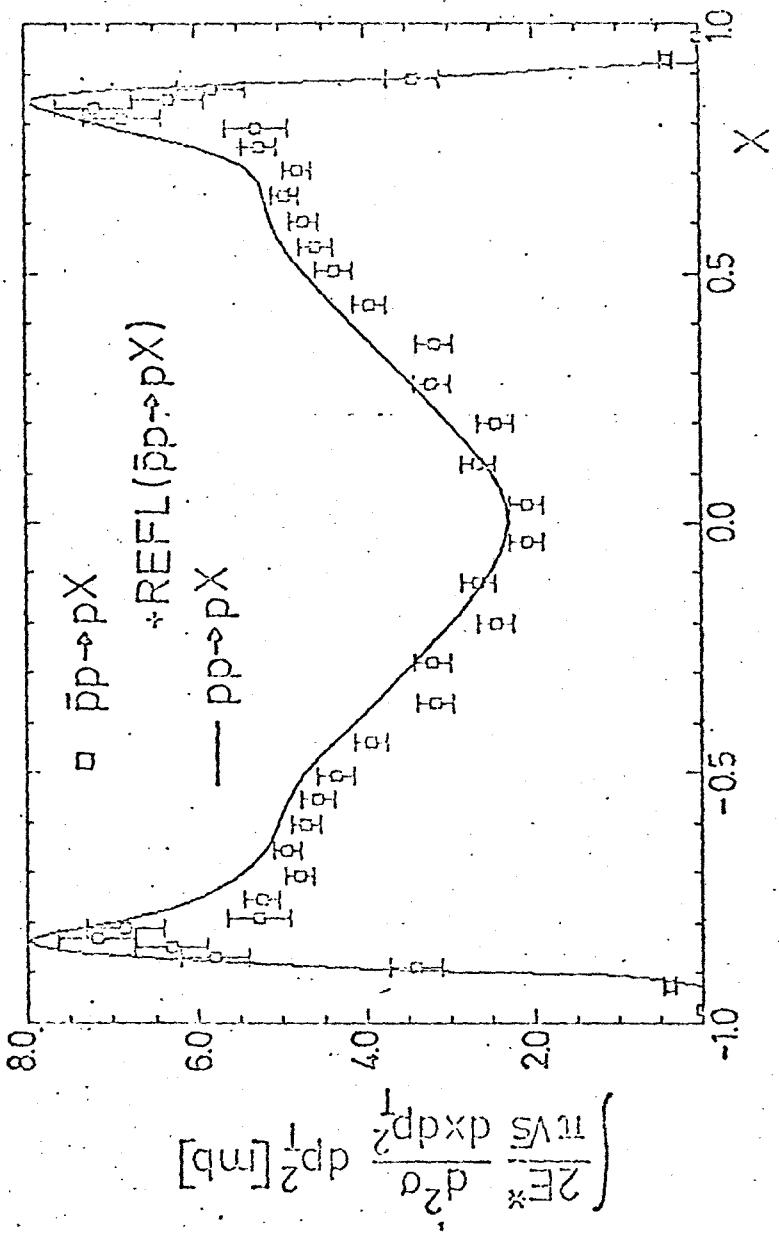
$\int \frac{2E^*}{\pi\sqrt{s}} \frac{d^2\sigma}{dx dp_T^2} dp_T^2$ [mb]
8.0
6.0
4.0
2.0
-1.0
-0.5
0.0
0.5
1.0
X
$\bar{p}p \to pX$
$pp \to pX$
$+ REFL(\bar{p}p \to pX)$

Fig. 4

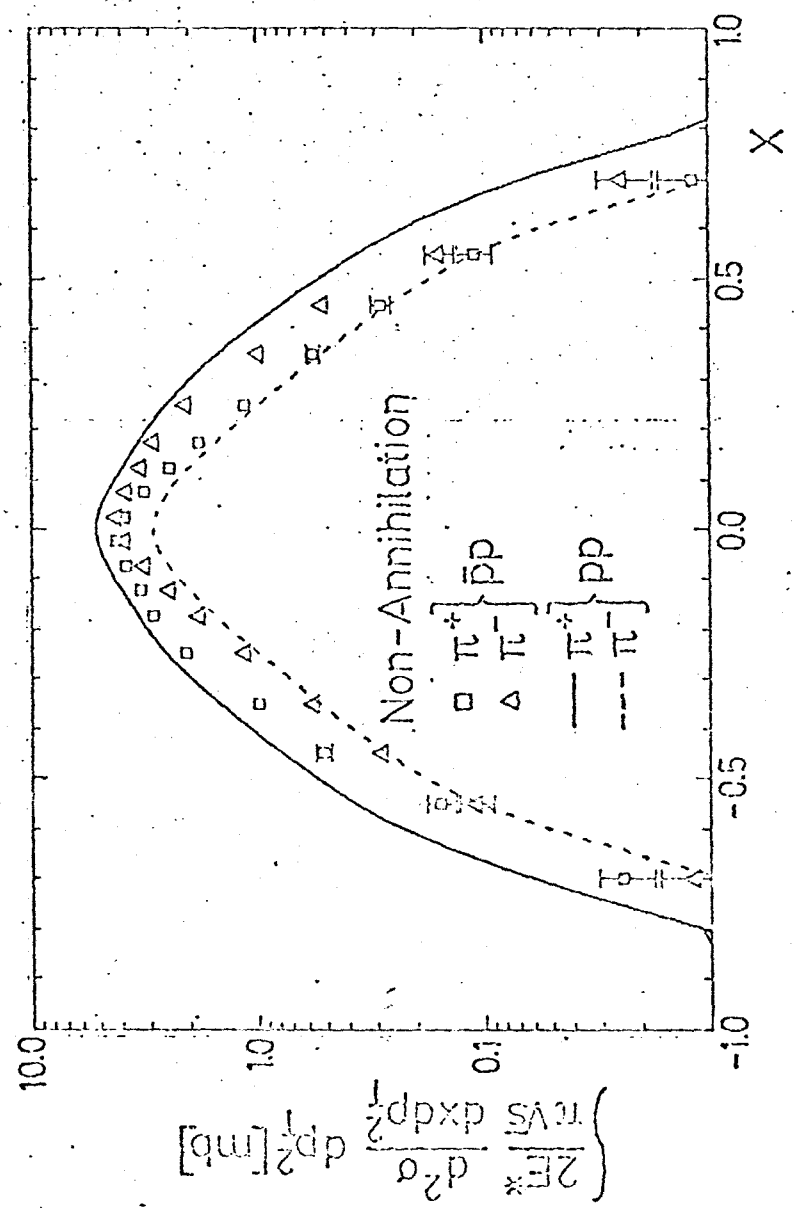
$\left\{\frac{2E^*}{\pi\sqrt{s}}\frac{d^2\sigma}{dx\,dp_t^2}\,dp_t^2[mb]\right.$
10.0
1.0
0.1
1.0
0.5
0.0
-0.5
-1.0
X
Non-Annihilation
$\bar{p}p$
π^+
π^-
pp
π^+
π^-

Fig. 5

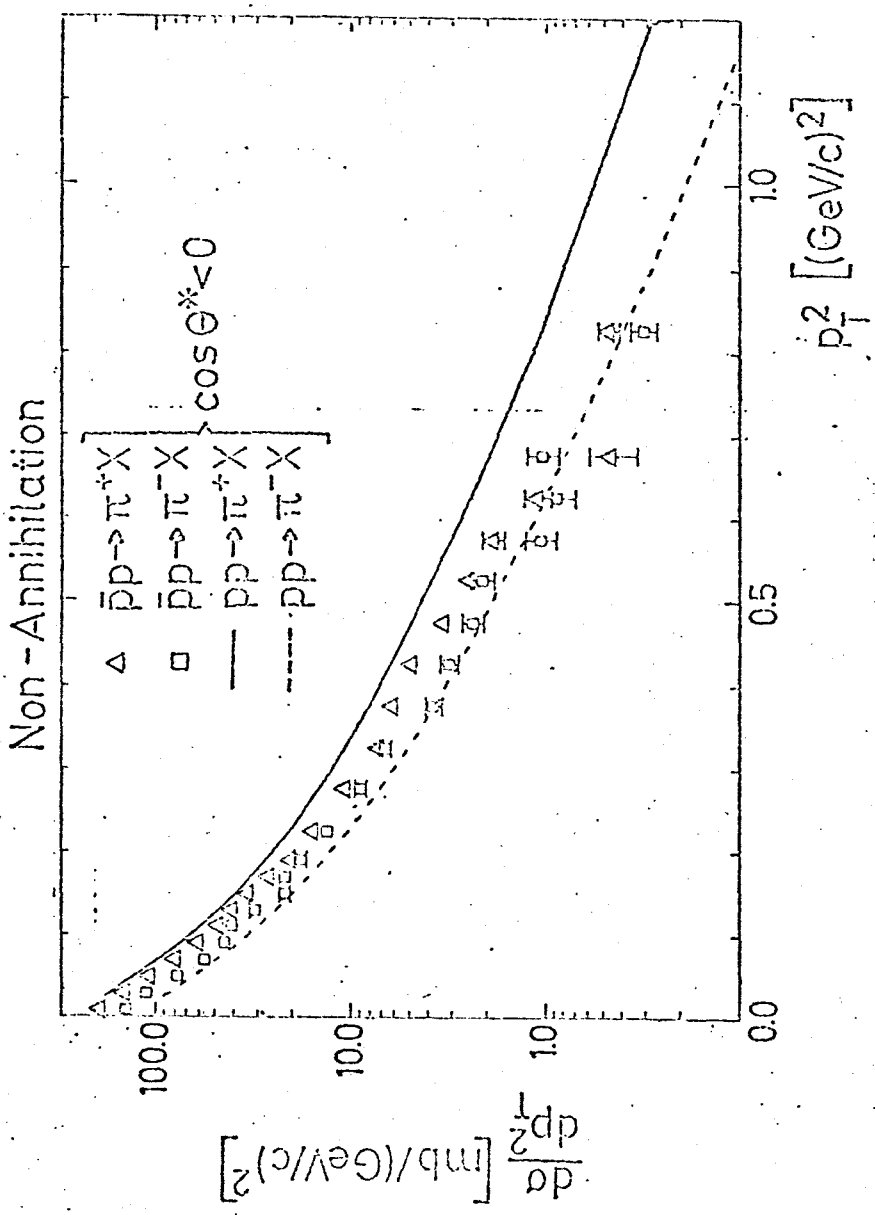
Non-Annihilation
$\bar{p}p \to \pi^+ X$
$\bar{p}p \to \pi^- X$
$pp \to \pi^+ X$
$pp \to \pi^- X$
$\cos\Theta^* < 0$
$\frac{d\sigma}{dp_T^2}$ [mb/(GeV/c)^2]
p_T^2 [(GeV/c)^2]
100.0
10.0
1.0
0.0
0.5
1.0

Fig. 6

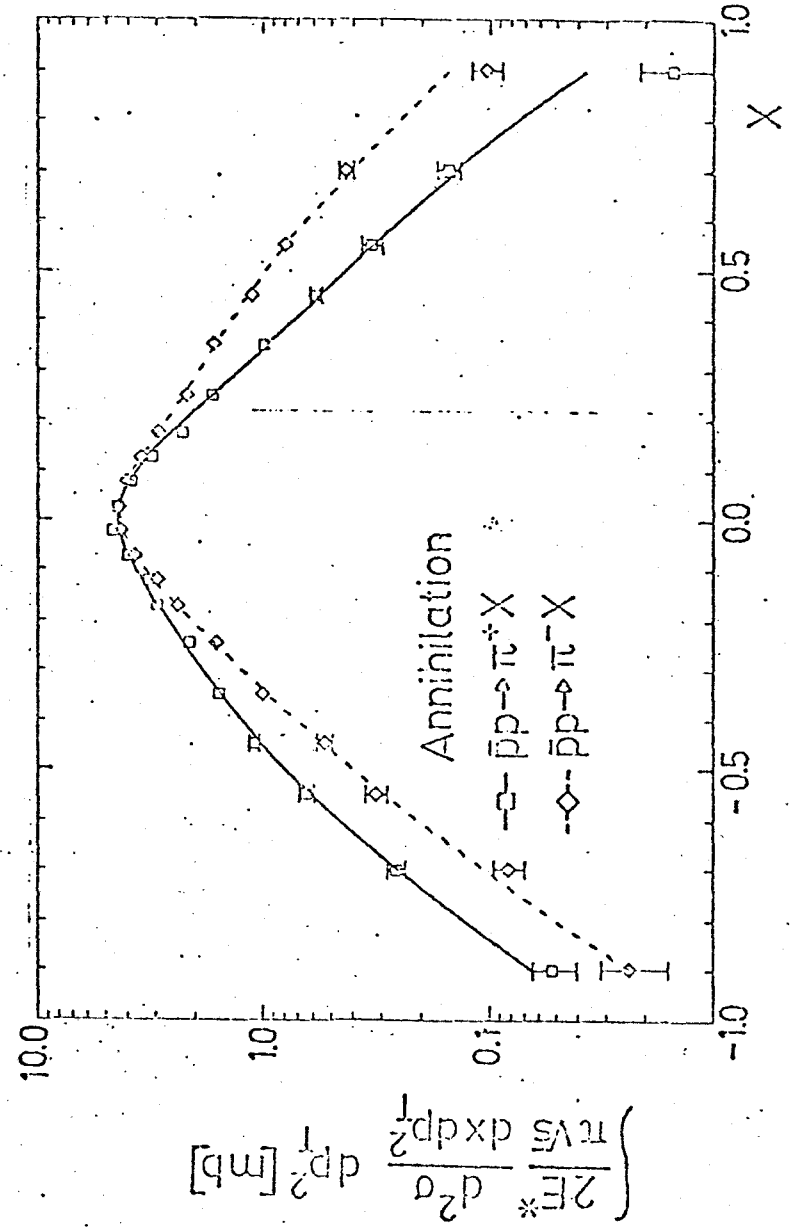
Annihilation
$\bar{p}p \to \pi^+ X$
$\bar{p}p \to \pi^- X$
$\int \frac{2E^*}{\pi\sqrt{s}} \frac{d^2\sigma}{dx\,dp_T^2}\, dp_T^2$ [mb]
X
10.0
1.0
0.1
-1.0
-0.5
0.0
0.5
1.0

Fig. 7

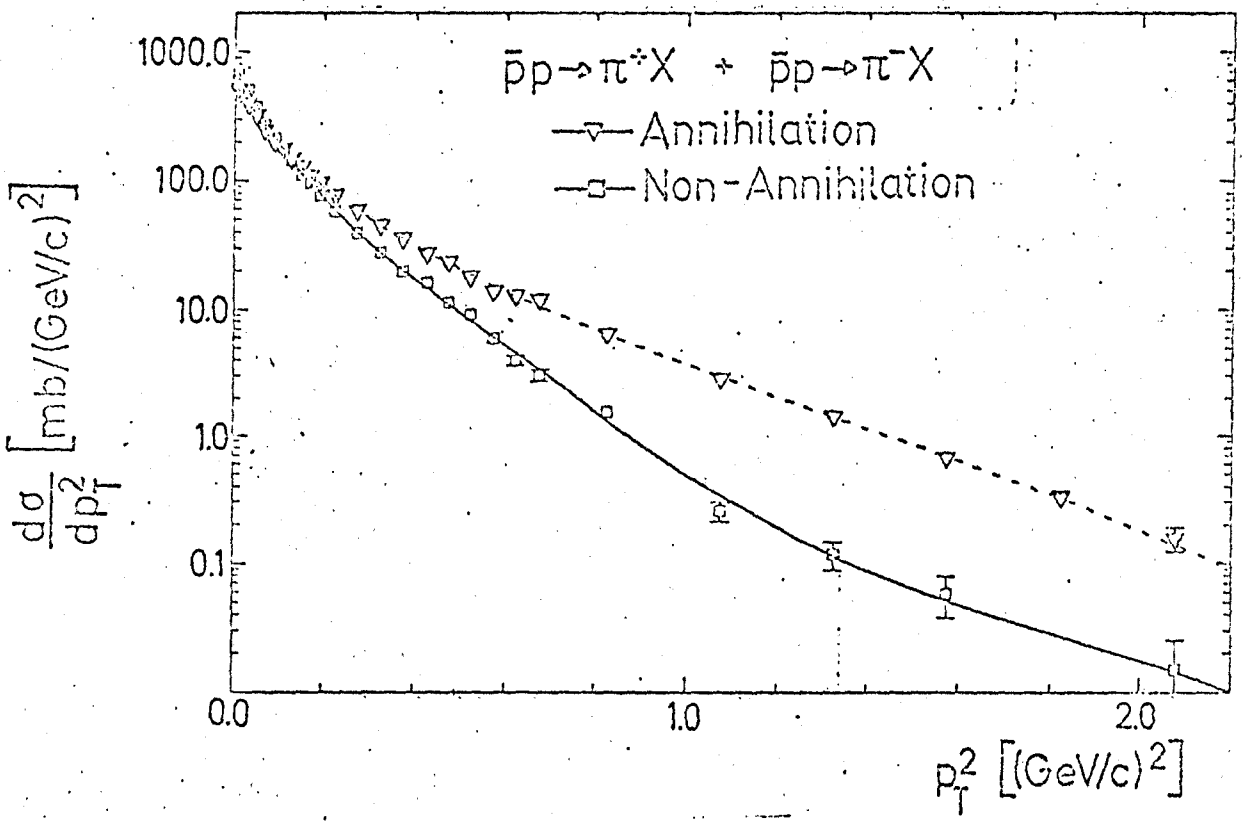
$\bar{p}p \to \pi^+ X + \bar{p}p \to \pi^- X$
Annihilation
Non-Annihilation
1000.0
100.0
10.0
1.0
0.1
0.0
1.0
2.0
$\frac{d\sigma}{dp_T^2}$ [mb/(GeV/c)^2]
p_T^2 [(GeV/c)^2]

Fig. 8

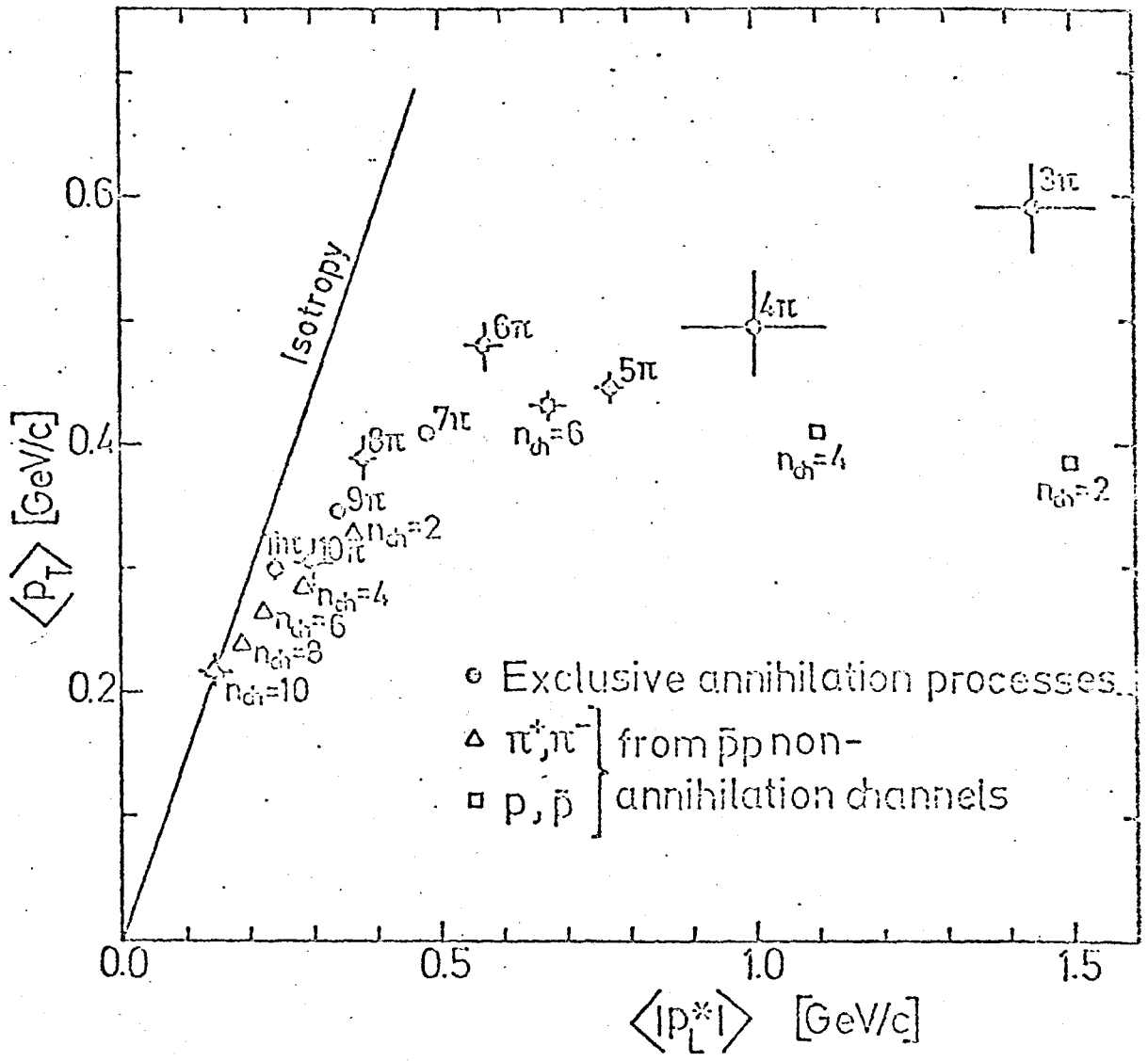
Isotropy
3π
4π
6π
5π
8π
7π
n_{ch}=6
n_{ch}=4
n_{ch}=2
9π
10π
n_{ch}=2
n_{ch}=4
n_{ch}=6
n_{ch}=8
n_{ch}=10
Exclusive annihilation processes
π^+,π^- from $\bar{p}p$ non-
p, $\bar{p}$ annihilation channels
0.0
0.5
1.0
1.5
0.2
0.4
0.6
$\langle p_T \rangle$ [GeV/c]
$\langle |p_L^*| \rangle$ [GeV/c]

Fig. 9

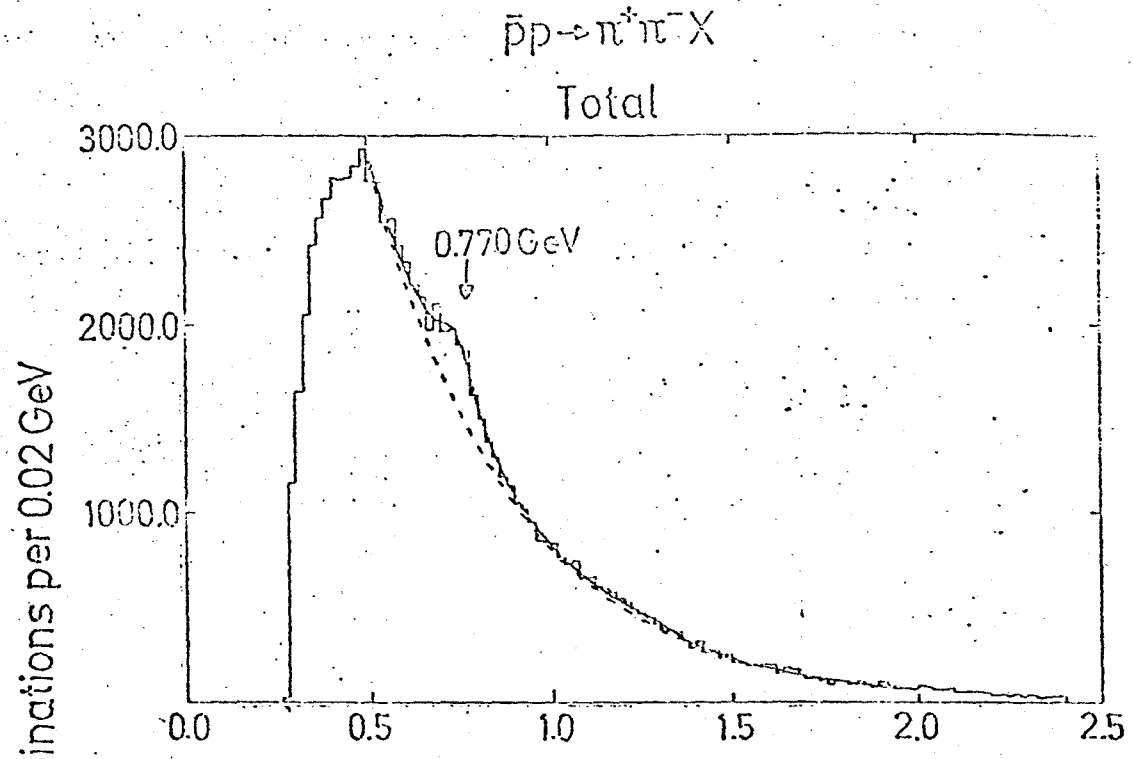

Fig. 10 a

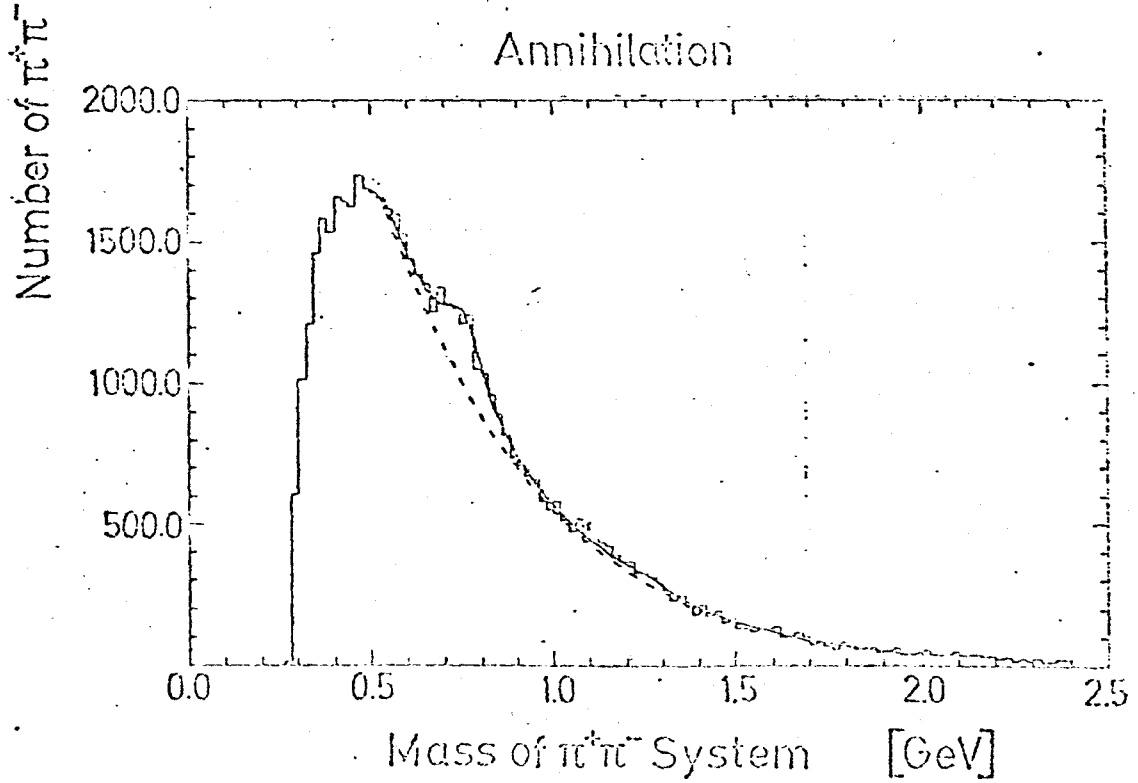

Fig. 10 b

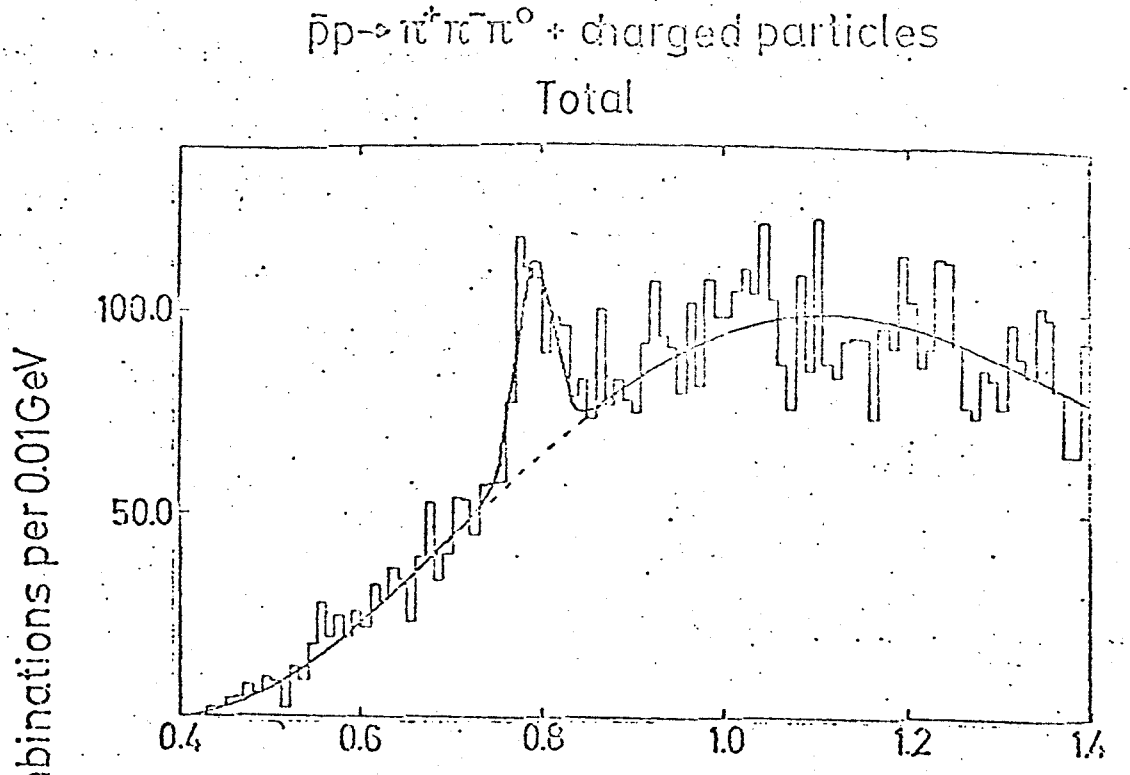

Fig. 11 a

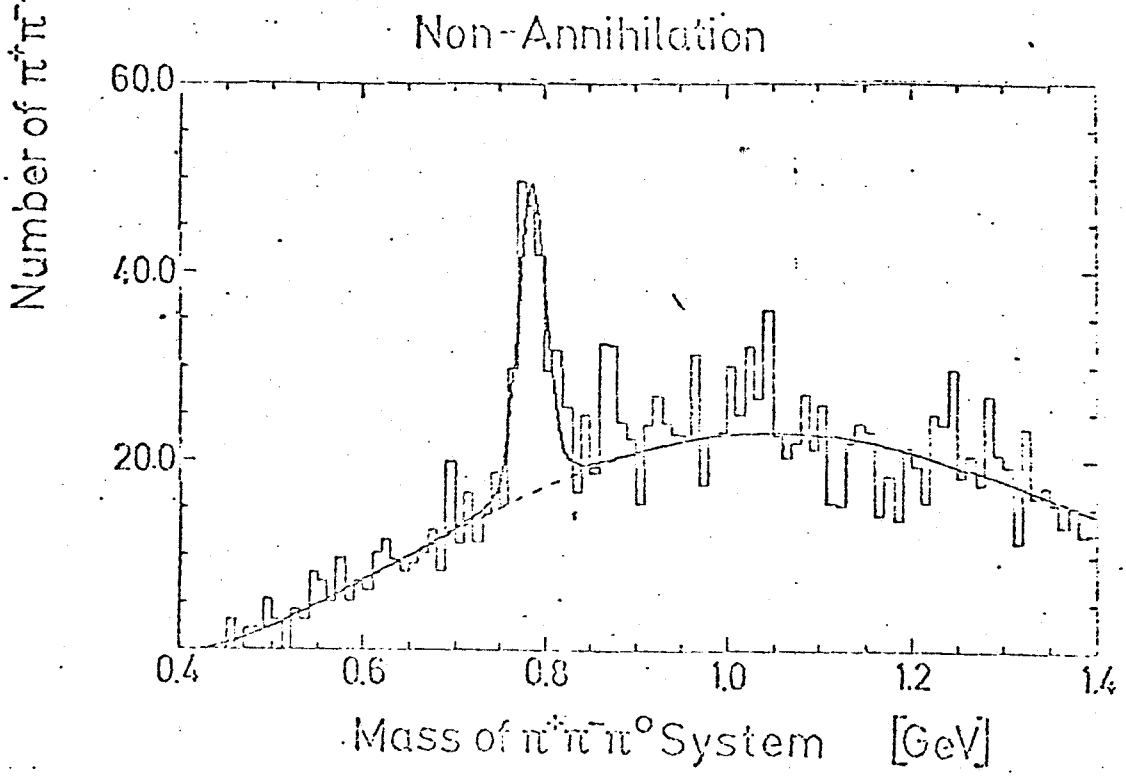

Fig. 11 b

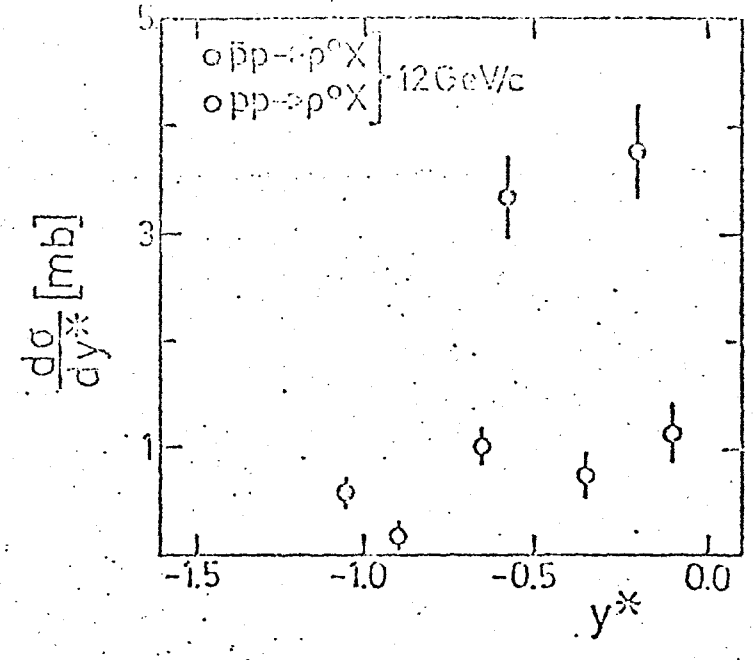

Fig. 12 a

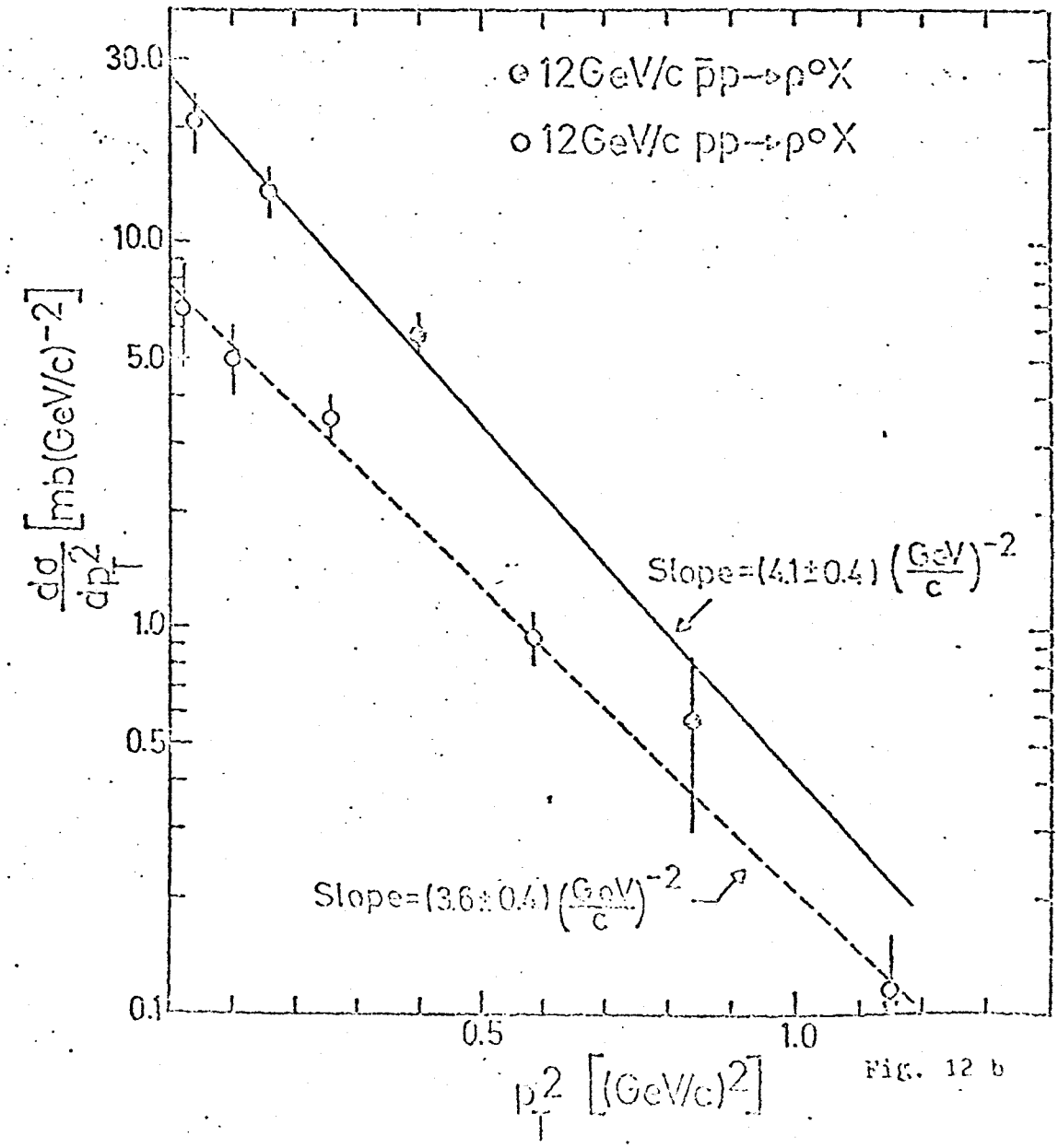

Fig. 12 b

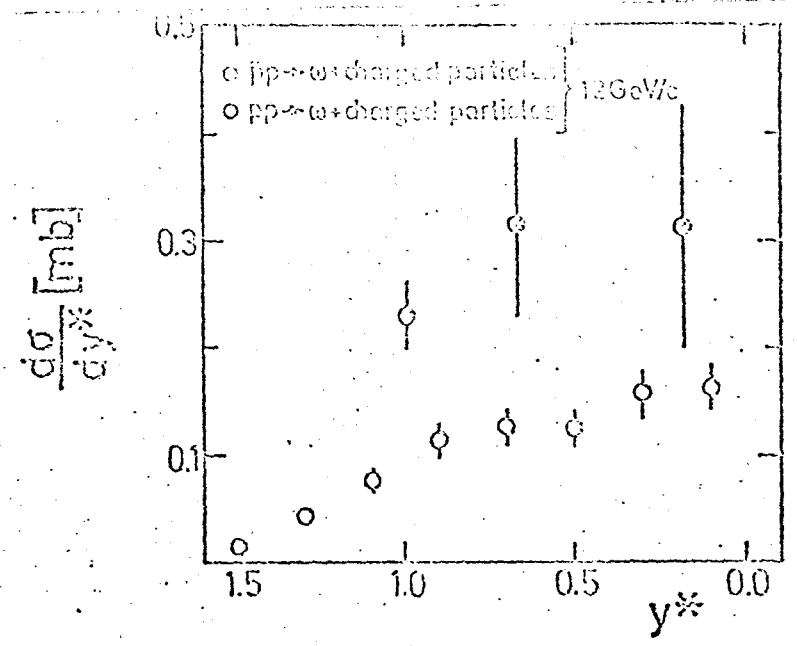

Fig. 13 a

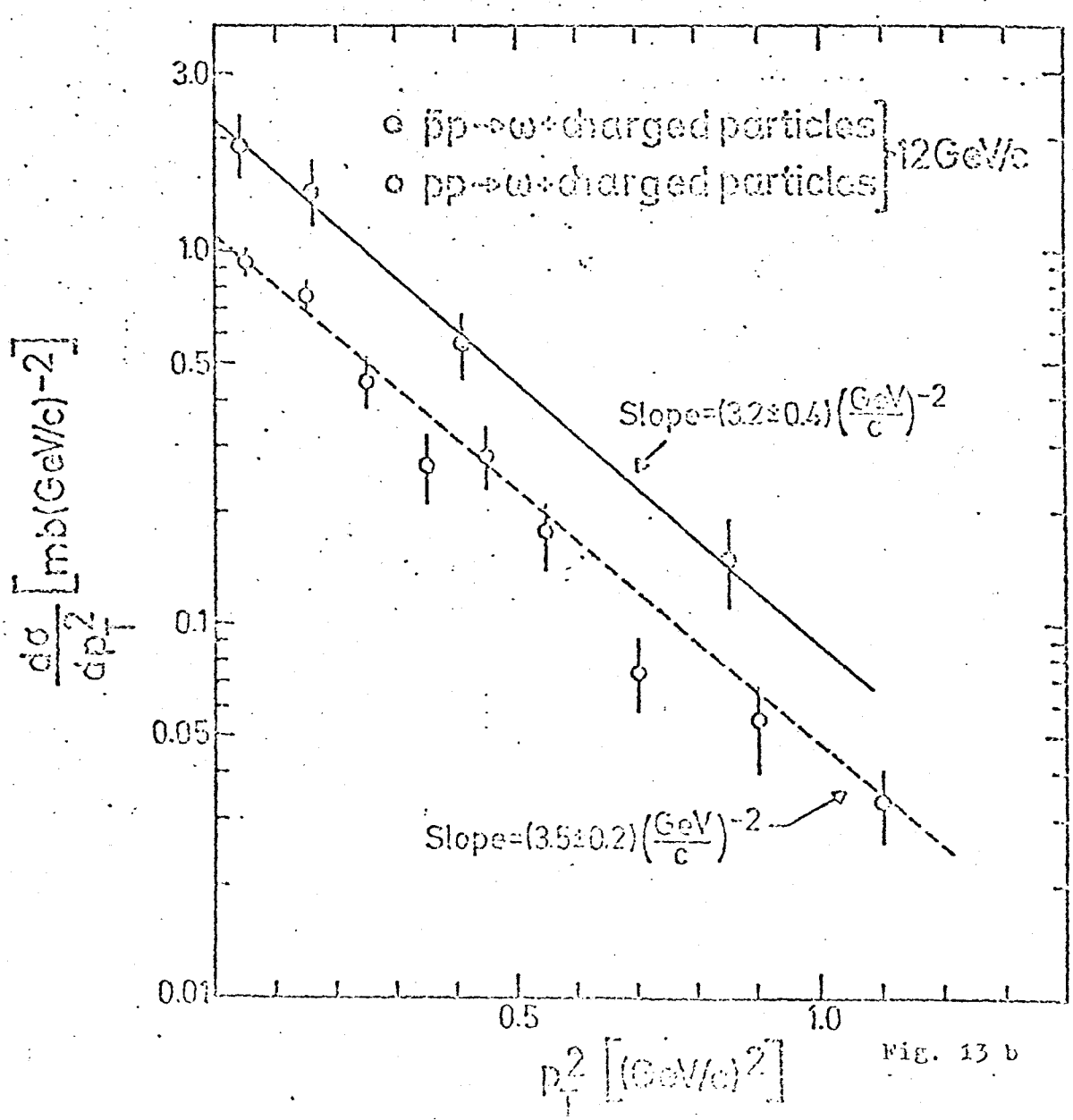

Fig. 13 b

Figure Captions

Fig. 1 Topological cross sections for inelastic $\bar{p}p$ and pp interactions at 12 GeV/c.

Fig. 2 Invariant cross section integrated over transverse momentum p_T for inclusive p production. Shown as a curve are the data for pp interactions.

Fig. 3 Invariant cross section for inclusive p production. Shown as curves are the data for pp interactions.

Fig. 4 Sum of p and $\bar{p}$ distributions. Shown as a curve is the p distribution for pp interactions.

Fig. 5 Invariant cross section integrated over transverse momentum p_T for inclusive non-annihilation π^+ and π^- production. Shown as curves are the data for pp interactions.

Fig. 6 Cross section for inclusive non-annihilation π^+ and π^- production as a function of p_T^2 . Shown as curves are the data for pp interactions.

Fig. 7 Invariant cross section integrated over transverse momentum for inclusive annihilation π^+ and π^- production. Curves are handdrawn to guide the eye.

Fig. 8 Cross section for inclusive π^+ and π^- production as a function of p_T^2 for annihilation and non-annihilation processes.

Fig. 9 Average value $\langle p_T \rangle$ of transverse momentum versus average value $\langle |p_L^*| \rangle$ of the absolute value of longitudinal momentum in the c.m. for annihilation in 3 to 11 pions and for non-annihilation final states with 2 to 10 charged particles; the straight line shows the dependence for isotropic emission of pions in the c.m.

Fig. 10 Distribution of effective mass of all $\pi^+\pi^-$ combinations for the total event sample (a) and for annihilation (b).

Fig. 11 Distribution of effective mass of $\pi^+\pi^-\pi^0$ combinations in quasi-inclusive final states for the total event sample (a) and for non-annihilation (b).

Fig. 12 Cross section for total inclusive ρ^0 production in $\bar{p}p$ and pp interactions as a function of rapidity y^* (a) and transverse momentum squared p_T^2 (b).

Fig. 13 Cross section for total quasi-inclusive ω production in $\bar{p}p$ and pp interactions as a function of rapidity y^* (a) and transverse momentum squares p_T^2 (b).

REFERENCES

1) I. Borecka et al., Nuovo Cimento 5 A (1971) 19;
G. Drews, Ph.D. Thesis, Internal Report DESY F1-71/7 (1974) (unpublished).

2) V. Blobel et al., Nuclear Physics B 69 (1974) 454.

3) G. Wetjen, Diploma Thesis, Internal Report DESY F1-74/3 (1974) (unpublished).

4) H.I. Miettinen, Symposium on Antinucleon-Nucleon Interactions , Report CERN 74-18 (1974) 405.

5) D. Everett et al., Symposium on Antinucleon-Nucleon Interactions, Report CERN 74-18 (1974) 510;
D. Everett et al., Nuclear Physics B 73 (1974) 449.

6) D. Everett et al., Nuclear Physics B 73 (1974) 440.

7) V. Blobel et al., Physics Letters 48 B (1974) 73.